JOURNAL OF Applied Polymer SCIENCE

Nitrofurazone-Loaded PVA–PEG Semi-IPN for Application as Hydrogel Dressing for Normal and Burn Wounds

Asheesh Gupta,[1] Nitin K. Upadhyay,[1] Surekha Parthasarathy,[2] Chitra Rajagopal,[2] Prasun K. Roy[2]

[1]Defence Institute of Physiology and Allied Sciences, Timarpur, Delhi 110054, India

[2]Centre for Fire, Explosive and Environment Safety, Brig. S. K. Majumdar Marg, Delhi 110 054, India

Correspondence to: P. K. Roy (E-mail: pk_roy2000@yahoo.com).

ABSTRACT: Hydrogels have been used in a wide variety of biomedical devises, particularly in the field of drug delivery, tissue engineering, and wound healing. In this study, a polyvinyl alcohol (PVA)–polyethylene glycol (PEG) semi-interpenetrating hydrogel network (IPN)-based wound dressing system containing nitrofurazone (NFZ) was synthesized by chemical crosslinking technique. The introduction of PEG to PVA matrix led to reduction in the water vapor transmission rate, which in-turn resulted in improved healing activity. Drug-loaded IPNs were prepared by mixing aqueous solution of NFZ with the optimized PVA–PEG formulation subsequent to the crosslinking step. The *in vitro* diffusion studies of NFZ indicated a relatively slow release of drug resulting from its microencapsulation in the polymeric matrix. Subsequently, *in vivo* wound healing efficacy toward acute and burn wound healing in experimental rats was investigated. Semi-IPN hydrogel loaded with NFZ dressing improved the overall healing rate in both acute and burn wounds, as evidenced by significant increase in total protein, hydroxyproline and hexosamine contents. Histological examinations also correlated well with the biochemical findings. A faster wound contraction was also observed in hydrogel treated acute and burn wounds. The results indicated that PVA–PEG semi-IPN hydrogel based dressing systems containing NFZ could be used as an effective wound dressing material. © 2012 Wiley Periodicals, Inc. J. Appl. Polym. Sci. 128: 4031–4039, 2013

KEYWORDS: biocompatibility; crosslinking; swelling; gels

Received 2 July 2012; accepted 17 September 2012; published online 17 October 2012

DOI: 10.1002/app.38594

INTRODUCTION

Wound management aims at rapid healing and epithelialization at the wound site to prevent infection and reduce functional and esthetic after effects. Currently, several research groups are working on the synthesis and modification of biocompatible materials with an aim to develop potential wound dressings, which can be employed in the management of burns, chronic and diabetic ulcers, etc.[1] Wound dressings can be broadly categorized into two types: dry and moist. It is widely accepted that the re-epithelialization rate of wound is much higher, when it is maintained under moist environments. In this context, special interest has been focused toward hydrogels, because of their unique characteristics which can meet the necessities of ideal wound dressings including immediate pain control, barrier against bacteria, absorption and prevention of body fluid loss, oxygen permeability, absence of antigenicity and toxicity, good handling and control of drug dosage.[2–4]

Polyvinyl alcohol (PVA) hydrogels have been used for several biomedical applications in the form of implants, artificial organs, contact lens, drug delivery devices, wound dressings, etc., because of its low toxicity and excellent biocompatibility.[5–7] Some of the common techniques employed to crosslink PVA include photo crosslinking,[8] freezing–thawing,[9,10] electron beam irradiation,[11] γ-irradiation,[12,13] and chemical crosslinking.[14] Our group has previously reported the wound healing ability of a chemically crosslinked PVA hydrogel prepared by reaction with potassium persulfate.[15] However, these hydrogels exhibited relatively high water vapor transmission rate (WVTR), the lowering of which is expected to improve its wound healing property. It was therefore, considered of interest to prepare blends with biocompatible polymers which could result in a reduction of WVTR.

Polyethylene glycol (PEG) is a nontoxic, water soluble polymer which resists recognition by the immune system.[16] It has also been reported to exhibit barrier properties against bacteria,[17] reduce the adsorption of proteins and deposition of cells thereby leading to rapid re-epithelialization. However, PEG exhibits inferior mechanical properties, which can be improved by blending with other mechanically strong polymers.[18] In this context, a semi-IPN network of silk fibroin and PEG has been studied as a wound dressing material.[19] In this study, we aim at

Table I. Compositional Details of Hydrogel Formulations

Sample designation	Amount (g)				Water (mL)
	PVA	$K_2S_2O_8$	PEG 600	NFZ	
PVA	10	-	-	-	100
PVA gel	10	0.5	-	-	100
IPN (PEG15)	10	0.5	1.5	-	100
IPN (PEG25)	10	0.5	2.5	-	100
IPN (PEG35)	10	0.5	3.5	-	100
IPN (PEG45)	10	0.5	4.5	-	100
IPN (PEG25-NFZ)	10	0.5	2.5	0.2	100
PVA gel-NFZ	10	0.5	-	0.2	100

developing a PVA–PEG semi-interpenetrating network and investigate its ability to heal acute and burn wounds.

To further improve the healing ability, the optimized semi-IPN formulation was loaded with nitrofurazone (NFZ), which has been reported to be an antibacterial, effective against a wide variety of Gram-negative and Gram-positive organisms.[20,21] NFZ exhibits bactericidal activity toward most pathogens that commonly cause surface skin infections, including *Staphylococcus aureus, Streptococcus, Escherichia coli, Clostridium perfringens, Enterobacter aerogenes*, and Proteus organisms.[22] In this study, both *in vitro* drug release and *in vivo* efficacy of the NFZ-loaded hydrogel toward healing of acute and burn wounds has been investigated.

EXPERIMENTAL

Materials

For the preparation of hydrogels, PVA (CDH, India) with a molecular weight of ~ 14,000, degree of saponification of > 99 mol %, 20 cp viscosity (4% aqueous solution) and PEG 600 (CDH, India) with average molecular weight of 570–630 was used, without further purification. All other chemicals including NFZ (5-nitro-2-furfural semicarbazone), Sigma-Aldrich, MO were used without any further purification. Mill-Q water was used throughout the course of the work.

Preparation of Semi-IPN PVA–PEG Hydrogel

The hydrogels were prepared by reacting PVA with potassium persulfate (0.5%, w/v) as described earlier.[15] A 10% w/v aqueous solution of PVA was prepared at 95°C using a rotary evaporator (Heidolph, Laborota-4003). PVA–PEG blends were prepared by adding PEG-600 in requisite amounts to the reaction mixture and allowing the reaction to proceed at 80°C for 150 min. The details of formulations along with their sample designations have been listed in Table I. The solution was subsequently transferred to a leveled Teflon tray and air-dried in a laminar flow hood to prepare films of ~ 1-mm thickness.

To prepare drug-loaded hydrogels, semi-IPNs containing 0.2%, w/v NFZ were prepared (Table I). Requisite amount of NFZ was added to the reaction mixture after cooling it to room temperature. The mixture was allowed to homogenize and subsequently poured into Teflon trays for drying.

Characterization of Hydrogels

Mechanical Properties. The mechanical properties of hydrogels, i.e., tensile strength and elongation at break were measured using a tensile strength testing machine (Jragrau Instruments, JRI-TT25). Five test specimens, each with a gauge length of 50 mm and width of 10 mm were cut from the swollen hydrogel sample and subjected to a crosshead speed of 50 mm/min, and the results have been expressed as mean ± SE.

Fourier Transform Infrared Spectroscopy

Fourier transform infrared (FTIR) spectrometry was carried out on a Perkin-Elmer Spectrum 2000 FTIR with an attenuated total reflectance (ATR) crystal accessory (Golden Gate). All spectra were calculated by means of 16 individual scans at 2 cm^{-1} resolution in the 4000–600 cm^{-1} interval with corrections for atmospheric water and carbon dioxide.

Thermal Analysis

The thermogravimetric analysis of dried hydrogel films was investigated using Perkin Elmer Diamond STG-DTA-DSC in N_2 atmosphere (flow rate = 200 mL/min) in the temperature range of 50–450°C. A heating rate of 10°C/min and sample mass of 3.0 ± 0.5 mg was used for each experiment. The calorimetric investigations were performed on Mettler-Toledo DSC instrument with a DSC 820 module. The sample (5.0 ± 0.5 mg) was heated at the rate of 10°C/min from 25 to 400°C under nitrogen atmosphere.

Swelling Behavior

For investigating the swelling behavior, the vacuum-dried films were immersed in excess water at room temperature (~ 30°C). Samples were removed at various intervals and weighed after removal of surface water with filter paper. The swollen gel was then slowly dried to constant weight. The equilibrium water content (EWC) was calculated according to the following formula.

$$\mathrm{EWC}\% = \left(\frac{W_s - W_d}{W_s}\right) \times 100\%$$

where W_s and W_d refer to the mass of the hydrogel in swollen and dry state, respectively.

Long-Term Stability of the Hydrogels

The long-term stability of developed hydrogels was determined as per procedure reported in literature.[23] The hydrogel samples were immersed in water at room temperature for extended time periods till 25 days. Aliquots of 5 mL from the solution were withdrawn and treated with 2.5 mL of 0.65*M* boric acid and 0.3 mL of 0.05*M* I_2/0.15*M* KI solution. This was diluted to 10 mL at 25°C and the absorbance of the greenish-blue PVA-iodine complex at 670 nm was measured to determine the concentration of free uncrosslinked PVA in the solution. Weight loss from the hydrogels was also investigated as a function of immersion time. For this purpose, the samples were removed at regular intervals, dried under vacuum and weighed.

Water Vapor Transmission Rate

Preliminary rapid de-swelling studies on the formulations were performed by thermogravimetry using a Perkin Elmer Diamond STG-DTA in flowing N_2 atmosphere (flow rate = 200 mL/min) under isothermal conditions (35°C). For this purpose, a known

mass of swollen hydrogel was placed in the crucible and allowed to reach equilibria over extended time periods.

After preliminary investigations, WVTR was determined as per the standard methodology (ASTM E 96). However, keeping in mind the end use of the hydrogel, the experiment was performed under an atmosphere of 32 ± 3% relative humidity (RH), maintained using saturated $MgCl_2$ solution at a temperature of 32°C as reported in the literature.[24] The test dish was filled up to two-third of its capacity with water and subsequently capped with the hydrogel specimen. The weight loss of this capped test dish was measured after 24 h and the WVTR was calculated using the following formula:

$$\text{WVTR\%} = \left(\frac{W_i - W_f}{A \times 24}\right) \times 100\%\text{g/m}^2\text{/h}$$

where WVTR is expressed in g/m^2/h, A is the area of test dish mouth (mm^2), W_i and W_f are the weight of capped test dish before and after 24 h of incubation under specified RH conditions, respectively.

Drug Release Behavior

Hydrogel samples of 8-mm diameter were cut out from the films and carefully transferred to empty polypropylene tubes containing 15.0-mL phosphate buffer saline (PBS; 0.1*M*, pH 7.4). At specified sample collection intervals, 1.0-mL solution was removed from test solution and transferred to a sample vial. The test solution was replenished with 1.0-mL fresh PBS. Duplicate hydrogel test samples were analyzed in each experiment. The concentration of NFZ released was determined by measuring the absorbance of the release solution at 365 nm using a UV spectrophotometer (BIORAD, USA).[21] A linear regression model of absorbance as a function of NFZ concentration was fitted, which was subsequently used for estimating the concentration of NFZ in release solutions. The mass released at time i (M_i) was calculated from the equation.[17,25]

$$M_i = C_i V + \sum C_{i-1} V_s$$

where C_i is the concentration of NFZ in the release solution at time i, V is the total volume of release solution, and V_s is the sample volume (1.0 mL).

In Vivo Wound Healing Tests

In this study, two set of experiments were carried out separately on acute and impaired burn wounds to evaluate the wound healing efficacy of the developed semi-IPN PVA–PEG hydrogels. Male Sprague-Dawley rats (180–200 g), from the animal colony of the DIPAS, Delhi, were used for this study. The experiments were performed in accordance with the regulations specified by the Institute's Animal Ethical Committee and conform to national guidelines on the care and use of laboratory animals. A total of 36 rats were divided into two groups of 18 rats each for acute and burn wound models. Further each group was subdivided in three subgroups of six rats each. Subgroup I being the control group treated with sterile cotton gauze dressing, Subgroup II being the experimental group treated with PVA–PEG blend and the last one (Subgroup III) containing the experimental group treated with NFZ incorporated PVA–PEG semi-IPN

All developed PVA–PEG semi-IPN hydrogels were sterilized by exposure to ethylene gas chamber (Steri-Vac 3M, Model 5XL Gas, MN) prior to animal experimentation. The saline imbibed hydrogels were applied on the excised wounds and maintained in position with the help of a microporous tape. The same was changed on a daily basis to monitor the wound healing process.

Acute Wound Model. The animals were anesthetized by intraperitoneal injection of thiopentone (25 mg/kg). The dorsal surface of the rat was shaved, and the underlying skin was cleaned with 70% ethanol. A 2 × 2 cm^2 open excision type of wound was created using scalpel blade to the depth of loose subcutaneous tissues, as described previously.[15] Animals were subsequently allowed to recover from anesthesia and housed individually in sterile cages.

Burn Wound Model. Full-thickness burn wound was created by using a metal rod (1.5-cm diameter) heated to 85°C. The temperature of the metal rod was monitored with a fabricated digital computerized multimeter. Hot rod was exposed at the shaved area of the rat for 20 s, resting on its own weight (30 g). No additional pressure was applied on the hand leaded metal rod. Single burn wound was created on dorsal part of each rat. After 24 h, dead tissues were excised using sterile surgical blade as per the established procedure.[26]

Evaluation of Prohealing Parameters. Wound surface area was measured by tracing its contour using a transparent paper on the 8th day before wound excision to monitor wound contraction. The area (mm^2) within the boundary was measured planimetrically as per the procedure reported previously.[15] The granulation tissue excised on 8th postwound day was used to analyze prohealing biochemical parameters viz. hydroxyproline,[27] hexosamine and total protein content.[28] The excised granulation tissues were also preserved in 10% neutral formalin for histopathological studies. The tissue sections of 6-μm thickness were stained with hematoxylin and eosin (H&E). Sections were assessed for the histological changes under light microscope in respect of inflammatory cells, collagen formation, angiogenesis, and epithelialization.

Statistical Analysis

The data have been expressed as mean ± SE, and statistical significance between experimental and control values was analyzed by ANOVA followed by Dunnett's test using Graph Pad Prism 2.01 (Graph Pad Software, La Jolla, CA). A P-value < 0.05 was considered statistically significant.

RESULTS AND DISCUSSION

Reaction Mechanism

The reaction mechanism of potassium persulfate with PVA has been schematically discussed previously.[15] The reaction has been proposed to proceed via the formation of intermediate SO_4^- free radicals, which generate tertiary radicals on the polymeric chain. These radicals recombine, leading to the formation of a chemically crosslinked network, which has the ability to swell in water due to the presence of hydrophilic hydroxyl groups. The rate of this reaction has been reported to follow first order

Applied Polymer SCIENCE

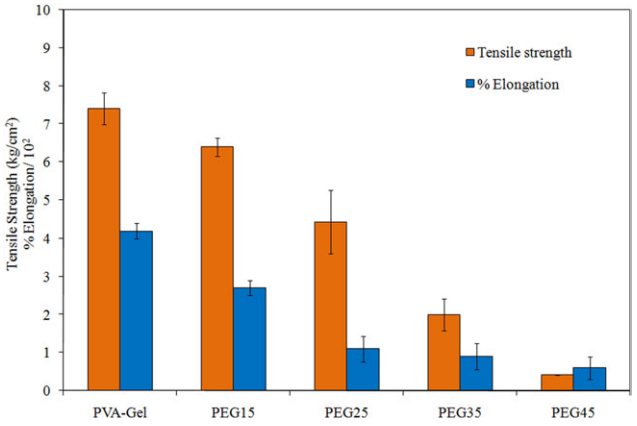

Figure 1. Effect of PEG on the tensile strength and elongation of PVA. [Color figure can be viewed in the online issue, which is available at wileyonlinelibrary.com.]

kinetics with respect of persulfate concentration and is proportional to the square root of PVA concentration.[29]

Under similar conditions, the reaction of PEG with potassium persulfate did not lead to crosslinking. This may be attributed to the fact that the reaction with PEG led to the formation of secondary radicals, which have much reduced stability as compared to the tertiary radicals formed in PVA. However, reaction of binary PVA–PEG solutions led to crosslinking and it can hence be concluded that the crosslinking reaction of PVA in the presence of PEG leads to the formation of semi-interpenetrating networks. However, at PEG concentrations of $> 35\%$, the crosslinking process was hindered, due to the inability of the tertiary radicals to recombine because of the steric hindrance offered by the interfering PEG chains. As a result, the resulting network is weak, which collapses during physical handling.

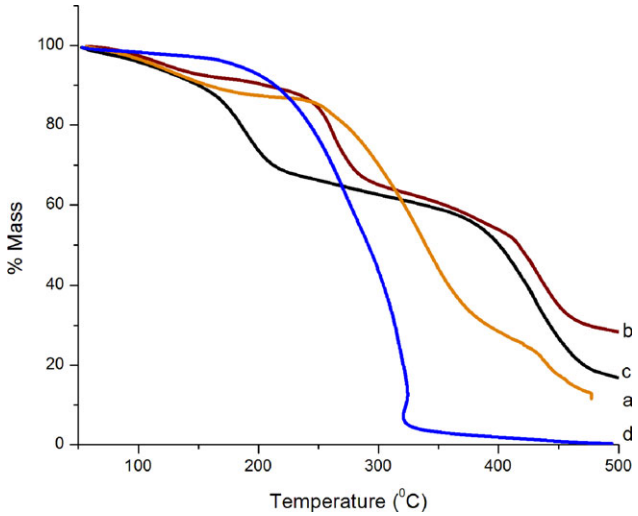

Figure 3. TGA traces (a) PVA, (b) IPN (PEG-25), (c) PVA-gel, and (d) PEG. [Color figure can be viewed in the online issue, which is available at wileyonlinelibrary.com.]

Characterization of PVA–PEG Semi-IPN Hydrogel

Mechanical Properties. The variation of mechanical properties of IPNs with increasing concentrations of PEG-600 is presented in Figure 1. Both the investigated mechanical properties, i.e. tensile strength, as well as elongation at break were found to depend adversely on the amount of PEG in the sample. Semi-IPN (PEG25) exhibited 40% and 7.4% reduction in tensile strength and elongation, respectively, as compared to neat PVA formulations. However, the mechanical properties of PEG25 remained unaltered on addition of NFZ. In fact, it was difficult to test formulations containing $> 35\%$ w/v PEG, as they disintegrated during physical handling.

Structural Characterization. FTIR spectra of PVA, PEG, PVA-gel, and IPN (PEG-25) are presented in Figure 2. Poly(ethylene glycol) exhibit characteristic absorption due to ether stretching

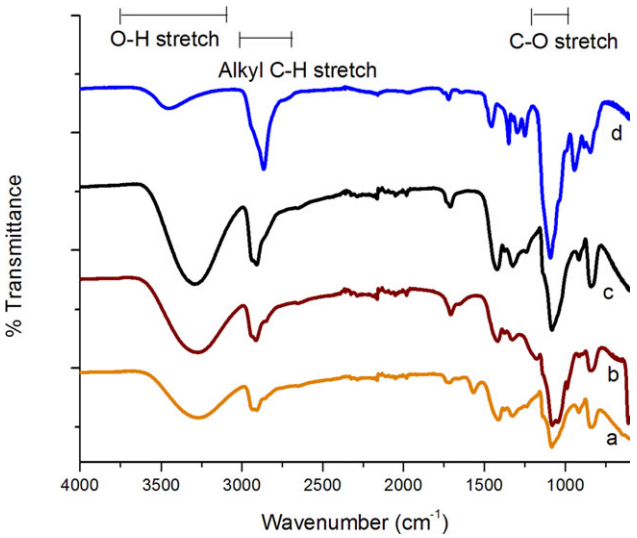

Figure 2. FTIR spectra of (a) PVA, (b) IPN (PEG-25), (c) PVA-gel, and (d) PEG. [Color figure can be viewed in the online issue, which is available at wileyonlinelibrary.com.]

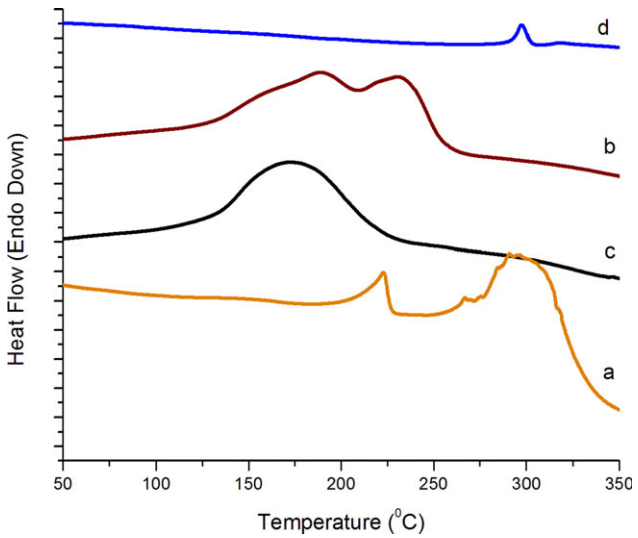

Figure 4. DSC traces (a) PVA, (b) IPN (PEG-25), (c) PVA-gel, and (d) PEG. [Color figure can be viewed in the online issue, which is available at wileyonlinelibrary.com.]

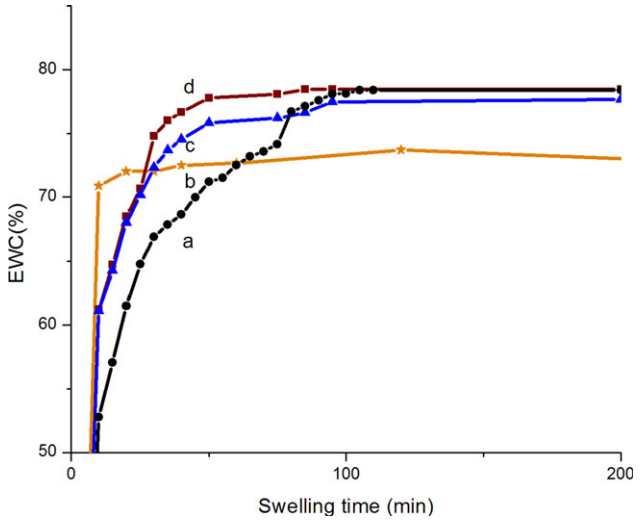

Figure 5. Variation of EWC (%) with immersion time (min). (a) IPN (PEG 35), (b) PVA-gel, (c) IPN (PEG 25), and (d) IPN (PEG 15). [Color figure can be viewed in the online issue, which is available at wileyonlinelibrary.com.]

bands from 1050 to 1150 cm^{-1}, with a maxima at 1150 cm^{-1}. Characteristic alkyl (R—CH_2) stretching at ~ 2850–3000 cm^{-1} can also be observed, along with hydroxyl group absorption ranging from ~ 3200 to 3600 cm^{-1}. The FTIR spectrum of PVA reveal a broad C—H alkyl stretching band (~ 2850–3000 cm^{-1}) and typical strong hydroxyl bands for free alcohol (nonbonded —OH stretching band at ~ 3600–3650 cm^{-1} and hydrogen bonded OH stretching at ~ 3200–3570 cm^{-1}).[30] The hydrogen band has contributions from both intramolecular and intermolecular bondings between the hydroxyl groups in the PVA chain. Another important absorption peak can be observed at ~ 1142 cm^{-1} (C—O, ~ 1090–1150 cm^{-1}), which is related to carboxyl

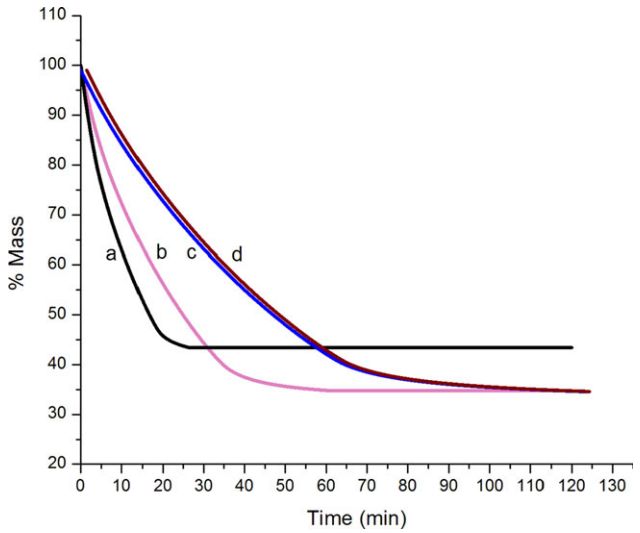

Figure 6. Isothermal thermogram's of swollen hydrogels. (a) PVA-gel, (b) IPN (PEG15), (c) IPN (PEG25), and (d) IPN (PEG25 NFZ). [Color figure can be viewed in the online issue, which is available at wileyonlinelibrary.com.]

Table II. WVTR of Developed Formulations

Sample designation	WVTR ($g/m^2/h$)[a]	WVTR ($g/m^2/h$)[b]
PVA gel	176.5 ± 1.5	20.0 ± 2.5
IPN (PEG15)	154.1 ± 2.3	19.3 ± 2.5
IPN (PEG25)	112.2 ± 10.4	14.1 ± 2.9
IPN (PEG35)	109.3 ± 3.4	14.2 ± 3.0
IPN (PEG25-NFZ)	110.2 ± 11.4	14.2 ± 2.7

[a]WVTR at 0% RH. WVTR at 32% RH.

stretching band (C—O). The reaction of PVA and PEG with persulfate did not lead to any perceptible changes in the FTIR spectra, besides an enhanced absorption peak at 1713 cm^{-1}, which can be attributed to the conversion of few hydroxyl groups to >C=O functionalities.

Thermal Analysis

TGA and the DSC traces of samples in nitrogen atmosphere are presented in Figures 3 and 4. PEG exhibits single step decomposition with an initial decomposition temperature (IDT) of 226°C. This pyrolytic decomposition is a result of random C—O and C—C scissions forming products like ethylene, formaldehyde, and acetaldehyde,[31] the removal of which leads to an endotherm in the DSC trace. A three-step degradation can be seen in the thermogram of the PVA. The first step (80–100°C) is due to the removal of physically trapped water in the polymer matrix. The second, more pronounced step (250–350°C) is a result of the rapid elimination of H_2O from the polymer chain, leading to the formation of a polyene. These unsaturated chains can recombine on further heating to form aromatic rings, which subsequently decompose in the third step at 425°C.[32] PVA exhibits a sharp melting at 229°C (DSC trace) and the percentage crystallinity was calculated to be 30.7%, (ΔH_{fus} = 155 J g^{-1} for 100% crystalline PVA).[33] Crosslinked polymers also exhibit three-step decomposition, the first step being removal of trapped water. However, the onset of the second step is markedly lower. The reaction of persulfate with PVA leads to the

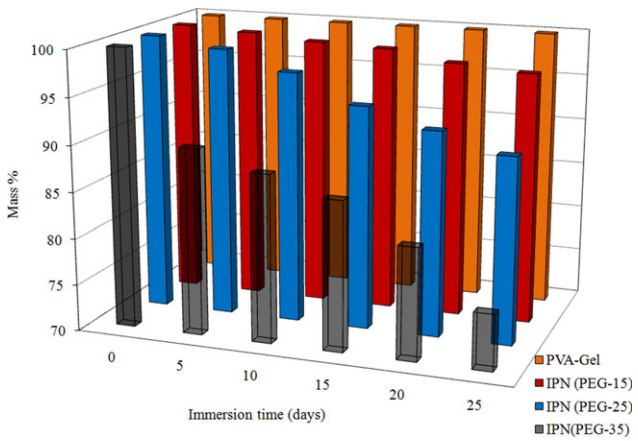

Figure 7. Weight loss of samples as a function of immersion time. [Color figure can be viewed in the online issue, which is available at wileyonlinelibrary.com.]

Applied Polymer SCIENCE

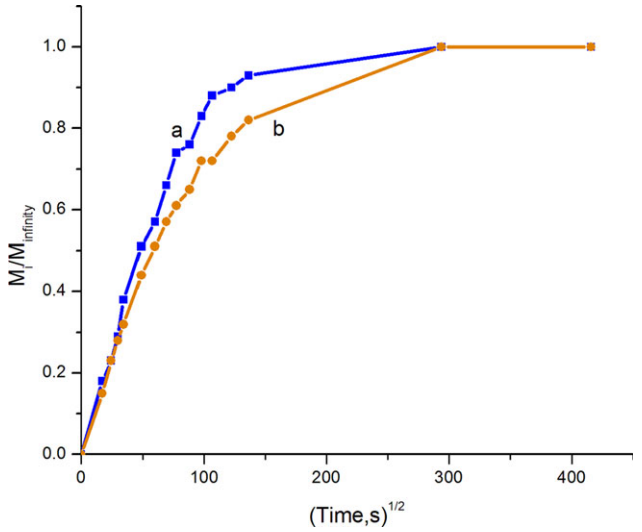

Figure 8. Diffusion of NFZ from hydrogel network as a function of release time. (a) PVA-NFZ and (b) IPN (PEG25 NFZ). [Color figure can be viewed in the online issue, which is available at wileyonlinelibrary.com.]

conversion of hydroxyl to carbonyl groups, resulting in the formation of a poly(ketone-*co*-alcohol) which exhibits a different thermal behavior with a reduced thermal stability as compared to the parent PVA macromolecule. The pyrolysis of this polymer can lead to formation of cyclic heterocyclic rings,[34] which decompose at a higher temperature in the third step. On the other hand, the presence of PEG interferes with the reaction of PVA with persulfate and therefore, the second step of degradation almost coincides with that of neat PVA. DSC traces reveal that all the crosslinked samples decompose before they can melt. The addition of NFZ into the polymer did not affect the thermal behavior of the hydrogel because of its presence at such low (0.2%) concentrations, and its TGA trace was identical to that of PEG25.

Swelling Behavior

The increase in the EWC (%) as a function of immersion time is presented in Figure 5. As is apparent from the figure, the prepared hydrogels absorbed water rapidly during the initial period and gained equilibrium within 20 min of immersion. It was observed that with the introduction of PEG, the uptake of water was relatively slower, however the EWC was higher. It is to be noted here that neat PVA films as well as samples containing high amounts of PEG (>35%) dissolved partially when placed in water and therefore their EWC could not be determined.

Water Vapor Transmission Rate

The thermogravimetric plots of swollen hydrogel formulations under isothermal conditions and flowing nitrogen atmospheres is presented in Figure 6. It can be seen that introduction of PEG led to a reduction in the rate of water vapor release. These preliminary investigations were followed by detailed WVTR studies and the transmission rates of developed formulations at both 32% and 0% RH are presented in Table II. From Table II, it can be seen that PVA based hydrogels exhibit a WVTR of $\sim$ 20.0 g/m^2/h. Introduction of PEG leads to a marked reduction in the WVTR of crosslinked PVA films. WVTR of some commercial wound dressings have been reported to lie in the range of 33–208 g/m^2/h.[35] Although there is no available ideal value of WVTR for wound dressings, but it is clear that the value must not be too high so to cause a dry condition in the wound area.[24] On the other hand, low WVTR would result in accumulation of exudates, which can open up risk for bacterial infection. It can be seen that increasing the amount of PEG-600 beyond 25% does not lead to any further decrease in WVTR, and based on the above analysis, semi-IPN (PEG 25) was investigated for its *in vivo* healing efficacy on experimental wounds. The optimum WVTR, as observed with semi IPN (PEG-25) leads to painless removal of the dressing which needs to be done at regular intervals for monitoring the wound healing process.

Long-Term Stability of Hydrogels

Chemically crosslinked PVA hydrogels (PVA gel) did not exhibit any soluble PVA content even after 25 days of water immersion. The mass loss profile of PVA-gel, PEG-15 and PEG-25 as a function of immersion time is presented in Figure 7. As expected, the IPNs exhibited mass loss when immersed in water, which was due to removal of uncrosslinked PEG from the polymer matrix. Interestingly, with increasing glycol concentration, the dissolution content of PVA also increased. The amount of soluble PVA present in the release solution was 0.5% for PEG-15, 0.9% for PEG-25, and 3% for PEG-35, which can be attributed to the fact that PEG interfered with the crosslinking reaction.

Drug Release from PVA–PEG Semi-IPN Hydrogel

For hydrogel containing 0.2% w/v NFZ, the M_i/M_∞ value was plotted as a function of the square root of release time ($t^{1/2}$) and the same has been presented in Figure 8. Diffusion studies revealed that NFZ, when added to water in small amounts gets

Table III. Effect of PVA–PEG Semi-IPN Hydrogel Dressings on Various Prohealing Parameters in Acute Wounds

Parameters	Control	PVA–PEG semi-IPN (PEG25)	PVA–PEG semi-IPN (PEG25-NFZ)
Protein (mg/g tissue wt.)	101.88 ± 5.31	138.03 ± 6.05*	114.47 ± 3.71
Hydroxyproline (mg/g tissue wt.)	22.24 ± 0.61	29.87 ± 1.51*	26.16 ± 0.64*
Hexosamine (mg/g tissue wt.)	0.71 ± 0.03	0.91 ± 0.02*	0.79 ± 0.04
% Wound area contraction 4-day	19.33 ± 1.03	54.10 ± 5.26*	37.00 ± 0.58*
% Wound area contraction 7-day	46.97 ± 2.08	74.90 ± 0.87*	73.33 ± 1.67*

Values are mean ± SE of six rats. *$P < 0.05$ compared with control.

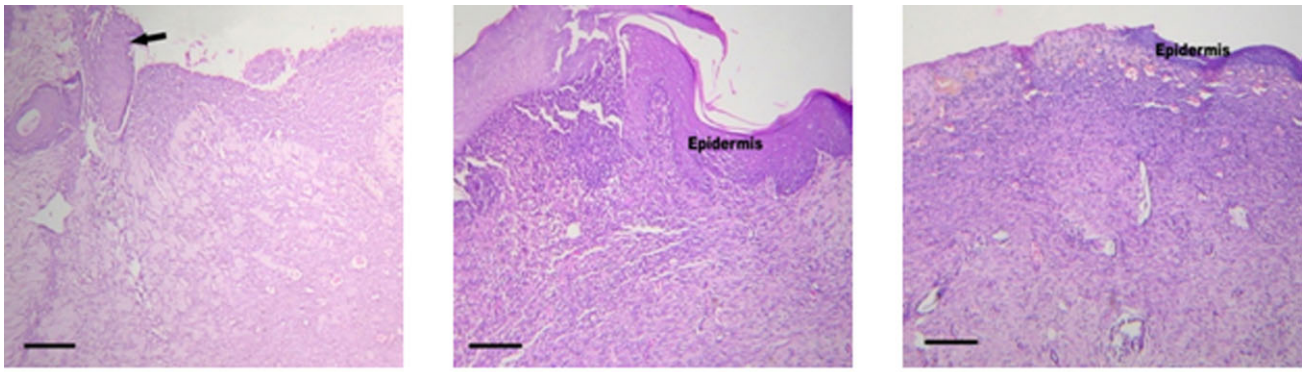

Figure 9. Histological section of the skin wound section of (a) normal wounds treated with sterile cotton gauze on 8th postwound day showing nonepithelialized wound surface with slight edema and congestion. Skin wound section of (b) PVA–PEG semi-IPN hydrogel and (c) NFZ incorporated PVA–PEG semi-IPN treated normal rats showing wound surface with well-organized thick epithelium and significant fibroblast and collagen deposition in deeper dermis. Neovascularization is well developed in PVA–PEG-treated normal rats (H&E, 100×, scale bar: 100 μm). [Color figure can be viewed in the online issue, which is available at wileyonlinelibrary.com.]

solubilized almost instantaneously (∼ 2 min). However, when the drug was encapsulated within the hydrogel, the release of NFZ was delayed, and from the figure, it can be concluded that most of the NFZ was released within 4 h. The introduction of PEG in the crosslinked polymeric matrix, did not lead to any significant change in the release pattern of NFZ.

Efficacy of Semi-IPN Hydrogel on Acute Wounds

The healing process for each wound treated by developed PVA–PEG semi-IPN hydrogel dressings progressed satisfactorily without any apparent complications. There were no evidences of infection or necrosis of wound, whereas skin was hemorrhagic for some controls and also exhibited presence of scab on the wound spot. During application control group showed hemorrhage by second damage while removing the gauze. It has been reported that crosslinked hydrogels have the ability to maintain moist environment around the wound area which is responsible for prevention of second damage during dressing changing.

The semi-IPN hydrogels treated wounds were found to contract much faster than the control group. Hydrogel treatment showed a significant augmented rate of wound contraction and prohealing biochemical parameters, which were also comparable with that of the NFZ incorporated semi-IPN hydrogel treated wounds (Table III). The histological examinations showed that tissue regeneration was much greater in the semi-IPN treated normal rats. Granulation tissue of the semi-IPN hydrogel treated wounds showed less inflammatory cells and reduced necrosis, which was present in control animals. The semi-IPN hydrogel treatment also enhanced fibroblast proliferation, angiogenesis and re-epithelialization (Figure 9).

Efficacy of Semi-IPN Hydrogel on Burn Wounds

Visual observation of the burn wound treated with semi-IPN hydrogel showed moist wound, with no clinical sign of inflammation or any pathological fluids oozing out from the wound margins. Untreated burn wounds exhibited pronounced edema, whereas wounds treated with hydrogel showed no or reduced edema. The semi-IPN hydrogel treated burn wound showed a significant reduction in wound area and increase in total protein, hydroxyproline and hexosamine content in the granulation tissues of experimental rats as compared to control group having gauze dressings (Table IV). The histological examinations revealed that tissue regeneration was much greater in wound treated with semi-IPN hydrogel without any signs of necrosis,

Table IV. Effect of PVA–PEG Semi-IPN Hydrogel Dressings on Various Prohealing Parameters in Burn Wounds

Parameters	Burn control	PVA–PEG semi-IPN (PEG25)	PVA–PEG semi-IPN (PEG25-NFZ)
Protein (mg/g tissue wt.)	95.91 ± 3.46	117.75 ± 4.21*	115.27 ± 1.90*
Hydroxyproline (mg/g tissue wt.)	18.51 ± 1.18	22.68 ± 1.89	24.86 ± 1.10*
Hexosamine (mg/g tissue wt.)	0.65 ± 0.02	0.77 ± 0.05	0.78 ± 0.02*
% Wound area contraction 4-day	22.16 ± 1.79	44.16 ± 2.91*	60.13 ± 3.17*
% Wound area contraction 7-day	48.99 ± 3.09	78.17 ± 0.98*	81.97 ± 2.01*

Values are mean ± SE of six rats. *$P < 0.05$ compared with burn control.

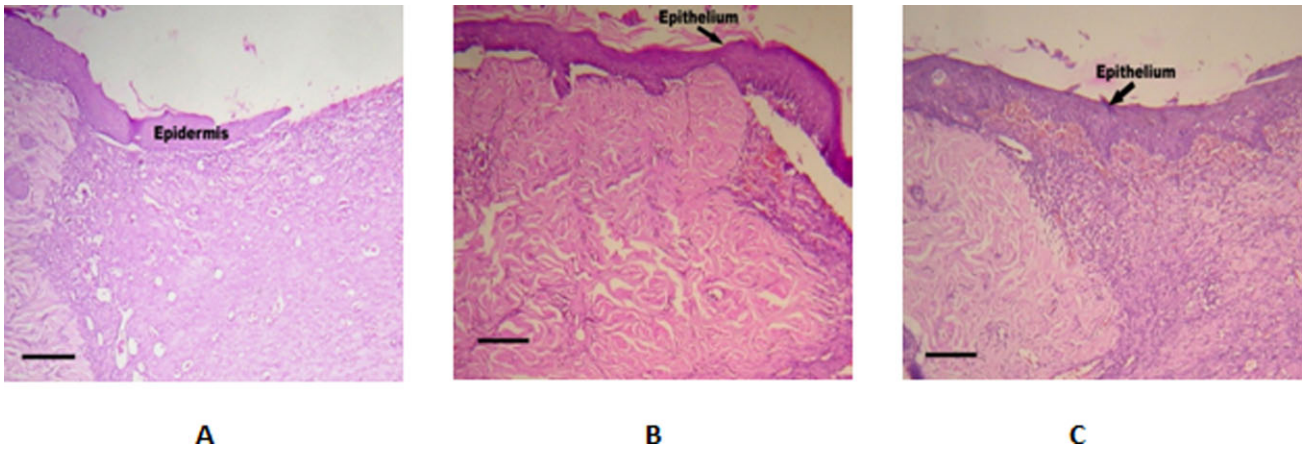

Figure 10. Histological section of the skin wound section of (a) control burn wounds treated with sterile cotton gauze showing presence of necrotic debris and incomplete epithelialization. (b) Skin wound section of burn wounds treated with PVA–PEG semi-IPN hydrogel showing greater degree of epithelialization, angiogenesis, and significant collagen deposition. (c) Skin wound section of NFZ incorporated PVA–PEG semi-IPN treated burn wounds (H&E, 100 ×, scale bar: 100 μm). [Color figure can be viewed in the online issue, which is available at wileyonlinelibrary.com.]

edema, congestion or inflammatory changes. More relative fibrosis and re-epithelialization were observed in hydrogel treated wounds (Figure 10).

CONCLUSIONS

The present investigation revealed that the developed NFZ-loaded PVA–PEG semi-IPN hydrogel possess several properties, which are essential for ideal wound dressings. The developed gels exhibited high elasticity, long-term stability and optimum water vapor transmission rate apart from having good mechanical strength. *In vitro* drug diffusion studies revealed that NFZ dissolved in water instantaneously, but post encapsulation in the hydrogel matrix, the same was released over a period of 4 h. The *in vivo* efficacy of the developed hydrogel toward both normal and burn wound healing was investigated, which revealed that the hydrogels were able to absorb body fluids effectively, apart from being soft in nature. These properties along with optimum WVTR values resulted in painless removal of the dressing, which is essential to aid the wound healing process. Thus, PVA–PEG semi-IPN loaded with NFZ could be used as an effective dressing material for acute as well as burn wound healing.

ACKNOWLEDGMENTS

The authors are thankful to Director, Defence Institute of Physiology and Allied Sciences, Delhi, India, and Director, Centre for Fire, Explosive and Environment Safety, Delhi, India, for their keen-interest and providing support to the study. N.K.U. is grateful to the Council of Scientific and Industrial Research (CSIR), New Delhi, India for the Senior Research Fellowship.

REFERENCES

1. Zahedi, P.; Rezaeian, I.; Ranaei-Siadat, S.-O.; Jafari, S.-H.; Supaphol, P. *Polym. Adv. Technol.* **2010**, *21*, 77.
2. Cascone, M. G.; Sim, B.; Downes, S. *Biomaterials* **1995**, *16*, 569.
3. Corkhill, P. H.; Hamilton, C. J.; Tighe, B. *J. Biomaterials* **1989**, *10*, 3.
4. Smith, A. G.; Din, A.; Denyer, M.; Crowther, N. J.; Eagland, D.; Vowden, K.; Vowden, P.; Britland, S. T. *Biotechnol. Progr.* **2006**, *22*, 1407.
5. DeMerlis, C. C.; Schoneker, D. R. *Food Chem. Toxicol.* **2003**, *41*, 319.
6. Kim, J. O.; Choi, J. Y.; Park, J. K.; Kim, J. H.; Jin, S. G.; Chang, S. W.; Li, D. X.; Hwang, M. R.; Woo, J. S.; Kim, J. A.; Lyoo, W. S.; Yong, C. S.; Choi, H. G. *Biol. Pharm. Bull.* **2008**, *31*, 2277.
7. Hong, K. H.; Sun, G. *J. Appl. Polym. Sci.* **2010**, *116*, 2418.
8. Bourke, S. L.; Al-Khalili, M.; Briggs, T.; Michniak, B. B.; Kohn, J.; Poole-Warren, L. A. *AAPS Pharmsci.* **2003**, *5*, 101.
9. Peppas, N. A.; Merrill, E. W. *J. Appl. Polym. Sci.* **1977**, *21*, 1763.
10. Hassan, C. M.; Peppas, N. A. *Macromolecules* **2000**, *33*, 2472.
11. Yoshii, F.; Zhanshan, Y.; Isobe, K.; Shinozaki, K.; Makuuchi, K. *Radiat. Phys. Chem.* **1999**, *55*, 133.
12. Wang, B. L.; Kodama, M.; Mukataka, S.; Kokufuta, E. *Polym. Gels Networks* **1998**, *6*, 71.
13. Nam, S. Y.; Nho, Y. C.; Hong, S. H.; Chae, G. T.; Jang, H. S.; Suh, T. S.; Ahn, W. S.; Ryu, K. E.; Chun, H. *J. Macromol. Res.* **2004**, *12*, 219.
14. Dai, W. S.; Barbari, T. A. *J. Membr. Sci.* **1999**, *156*, 67.
15. Gupta, A.; Kumar, R.; Upadhyay, N. K.; Surekha, P.; Roy, P. K. *J. Appl. Polym. Sci.* **2009**, *111*, 1400.
16. Yates, C. C.; Whaley, D.; Babu, R.; Zhang, J. Y.; Krishna, P.; Beckman, E.; Pasculle, A. W.; Wells, A. *Biomaterials* **2007**, *28*, 3977.
17. Leach, J. B.; Schmidt, C. E. *Biomaterials* **2005**, *26*, 125.
18. Iza, M.; Stoianovici, G.; Viora, L.; Grossiord, J. L.; Couarraze, G. *J. Controlled Release* **1998**, *52*, 41.

19. Kweon, H. Y.; Park, S. H.; Ye, J. H.; Lee, Y. W.; Cho, C. S. *J. Appl. Polym. Sci.* **2001**, *80*, 1848.
20. Munster, A. M. *J. Trauma-Injury Infec. Crit. Care* **1984**, *24*, 524.
21. Kim, J. O.; Park, J. K.; Kim, J. H.; Jin, S. G.; Yong, C. S.; Li, D. X.; Choi, J. Y.; Woo, J. S.; Yoo, B. K.; Lyoo, W. S.; Kim, J. A.; Choi, H. G. *Int. J. Pharm.* **2008**, *359*, 79.
22. Murugasu-Oei, B.; Dick, T. *J. Antimicrob. Chemother.* **2000**, *46*, 917.
23. Joshi, D. P.; Lanchunfung, Y. L.; Pritchard, J. G. *Anal. Chim. Acta* **1979**, *104*, 153.
24. Wu, P.; Fisher, A. C.; Foo, P. P.; Queen, D.; Gaylor, J. D. S. *Biomaterials* **1995**, *16*, 171.
25. Varshosaz, J.; Koopaie, N. *Iran. Polym. J.* **2002**, *11*, 123.
26. Upadhyay, N. K.; Kumar, R.; Mandotra, S. K.; Meena, R. N.; Siddiqui, M. S.; Sawhney, R. C.; Gupta, A. *Food Chem. Toxicol.* **2009**, *47*, 1146.
27. Woessner, J. F. *Arch. Biochem. Biophys.* **1961**, *93*, 440.
28. Lowry, O.; Rosebrough, N. J.; Farr, A. L.; Randall, R. J. *J. Biol. Chem.* **1951**, *193*, 265.
29. Ikada, Y.; Nishizaki, Y.; Sakurada, I. *J. Polym. Sci.: Polym. Chem. Ed.* **1974**, *12*, 1829.
30. Mansur, H. S.; Orefice, R. L.; Mansur, A. A. P. *Polymer* **2004**, *45*, 7193.
31. Fares, M. M.; Hacaloglu, J.; Suzer, S. *Eur. Polym. J.* **1994**, *30*, 845.
32. Yang, C. C. *J. Membr. Sci.* **2007**, *288*, 51.
33. Probst, O.; Moore, E. M.; Resasco, D. E.; Grady, B. P. *Polymer* **2004**, *45*, 4437.
34. Perez-Foullerat, D.; Hild, S.; Mucke, A.; Rieger, B. *Macromol. Chem. Phys.* **2004**, *205*, 374.
35. Razzak, M. T.; Darwis, D.; Sukirno, Z. *Radiat. Phys. Chem.* **2001**, *62*, 107.